

The Human $\Delta 1261$ Mutation of the *HERG* Potassium Channel Results in a Truncated Protein That Contains a Subunit Interaction Domain and Decreases the Channel Expression*

(Received for publication, June 24, 1996, and in revised form, October 1, 1996)

Xiaodong Li, Jia Xu, and Min Li^{‡§}

From the Department of Physiology and [‡]Department of Neuroscience, The Johns Hopkins University School of Medicine, Baltimore, Maryland 21205

***HERG* (human *eag*-related gene) encodes an inward-rectifier potassium channel formed by the assembly of four subunits. Since the truncated *HERG* protein in patients with long QT syndrome induces a dominant phenotype, that is, cardiac sudden death, the assembly of nonfunctional complexes between wild-type and mutated subunits was implicated in causing the disease. To understand *HERG*-mediated cardiac sudden death at the molecular level, it is important to determine which regions in the *HERG* protein participate in subunit interaction. We therefore report the identification of a subunit interaction domain, NAB_{*HERG*}, that is localized at the hydrophilic cytoplasmic N terminus and can form a tetramer in the absence of the rest of the *HERG* protein. Truncated *HERG* proteins containing NAB_{*HERG*}, including one that resulted from the $\Delta 1261$ human mutation, inhibit the functional expression of the *HERG* channel in transfected cells. Together, these results support the notion that the expression of *HERG* in the human heart may be decreased in the presence of the truncated subunit. Such a decrease of potassium channel expression can contribute to the longer QT intervals observed in the patients with the *HERG* mutation.**

Human *eag*-related gene (*HERG*) was first cloned on the basis of its homology to the *Drosophila ether a go-go* (*eag*) channel (1), a member of the *eag* potassium (K⁺) channel family. This group of proteins contains six putative transmembrane segments that are flanked by the cytoplasmic N-terminal and C-terminal domains (2, 3). Despite its overall topological similarity to the *eag* and Shaker-like outward K⁺ channels,

electrophysiological studies have shown that *HERG* subunits form inward-rectifier K⁺ channels (4, 5), which are generally made up of a different class of K⁺ channel subunits with only two transmembrane segments (6). In contrast to the Shaker-like channels, little is known about the region or regions that mediate the subunit assembly for either *eag* or inward-rectifier K⁺ channels.

Recently, *HERG* mutations were found in patients with chromosome 7-linked long QT syndrome, and it was proposed that the *HERG* dysfunctions caused cardiac arrhythmia (7). Because the biophysical properties of the *HERG* channel expressed in *Xenopus* oocytes resemble a well-characterized, rapidly activating, delayed-rectifier K⁺ current (also called I_{Kr}) found in cardiac myocytes (8), *HERG* probably encodes subunits of cardiac I_{Kr} channels. Since a decrease in I_{Kr} current could induce the longer interval typical of that seen in patients with long QT syndrome, it was proposed that the dominant disease phenotype could result, at least in part, from the non-functional subunit assembly of the mutated *HERG* protein with its compatible functional subunits (9). Thus, identifying the region or regions in the *HERG* protein involved in subunit interaction may help us understand the cause of chromosome 7-linked long QT syndrome at the molecular level.

EXPERIMENTAL PROCEDURES

Vector Construction—Expression of the glutathione *S*-transferase (GST)¹ fusion protein was carried out using pGEX-4T2 vector (Pharmacia Biotech Inc.). Vectors in which exogenous gene expression was driven by human cytomegalovirus (CMV) immediate early promoter were used to carry out all transient transfection experiments, and standard recombinant DNA techniques (10, 11) were used for plasmid vector construction. The vectors that express partial cDNA fragments were constructed by the high fidelity polymerase chain reaction cloning strategy that we have previously described (12). The NAB_{*HERG*} coding sequence was obtained by using ML1095 (GGGTCGACAATGCCGGT-GCGGAGG) and ML1129 (CAGGCGGCCGCTACTTCTCCATCAC-CACC) primers. The coding sequence for N-Herg was obtained by using ML1103 (CAGGAATTCCTCAGGATGCCGGTGC) and ML1104 (CAGGAATTCGGTGGATGCCGGTGC) primers.

The CMV promoter in the pRc/CMV vector (Invitrogen) was used to express cDNAs encoding the N-terminal domain of *HERG* (or N-Herg) and $\Delta 1261$. In the N-Herg expression vector, 12CA5 monoclonal epitope (PYDVPDYASL) was fused to the C terminus, while for $\Delta 1261$, 12CA5 monoclonal epitope was added to the N terminus. The expression vector for intact *HERG* was constructed by first releasing the *HERG* full-length cDNA from pSP64.HERG (from Dr. Mark Keating, University of Utah) (7, 8) with *Hind*III and *Eco*RI restriction enzymes. The cDNA fragment was then subcloned into the pRc/CMV vector (Invitrogen).

Construction of the $\Delta 1261$ Mutation—The $\Delta 1261$ mutation was constructed by a polymerase chain reaction-based mutagenesis strategy. The *HERG* coding sequence was amplified by 5'-ML1124 and 3'-ML1125 primers. The 3'-primer (CAGGGATCCTCAGCAGGAAGG-CAGCCGAGTAGGGTGTGAAGACAGCCGGTAGATGACCAGC) contains a single-base deletion at a position corresponding to position 1261 in *HERG*. Thus, the resultant fragment encodes a protein with an amino acid sequence equivalent to that of $\Delta 1261$.

Fusion Protein Expression and Purification—Fusion proteins and thrombin cleavage were obtained by standard protocol for GST fusions provided by manufacturer (Pharmacia Biotech Inc.).

Gel Filtration Chromatography—Protein in 0.5 M NaCl was separated by FPLC on Superdex-200 in a running buffer containing 20 mM HEPES pH 7.5, 500 mM NaCl, 2 mM EDTA, 1 mM 2-mercaptoethanol, and 0.5 mM phenylmethylsulfonyl fluoride. In a typical separation, 100

* This work was supported in part by grants from the National Institutes of Health, the Council for Tobacco Research-U.S.A., Inc., and a grant-in-aid from the American Heart Association (to M. L.). The costs of publication of this article were defrayed in part by the payment of page charges. This article must therefore be hereby marked "advertisement" in accordance with 18 U.S.C. Section 1734 solely to indicate this fact.

§ Neuroscience Fellow of the Alfred P. Sloan Foundation and the Esther A. & Joseph Klingenstein Fund. To whom correspondence should be addressed: Dept. of Physiology, The Johns Hopkins University School of Medicine, 725 N. Wolfe St., WBSB 216, Baltimore, MD 21205. Tel.: 410-614-3692; Fax: 410-614-1001; E-mail: min_li@qmail.bs.jhu.edu.

¹ The abbreviations used are: GST, glutathione *S*-transferase; CMV, cytomegalovirus; FPLC, fast performance liquid chromatography; PAGE, polyacrylamide gel electrophoresis.

μg of protein in 200 μl of running buffer was loaded. The column was developed at a flow rate of 0.5 ml/fraction/min.

Chemical Cross-linking—Purified fusion protein in a buffer containing 20 mM HEPES pH 7.5, 100 mM KCl, 2 mM EDTA, and 1 mM 2-mercaptoethanol was subjected to chemical cross-linking experiments using glutaraldehyde. The reaction was initiated by mixing an identical amount of protein (1 μg in 20 μl) with a stock solution of glutaraldehyde to a final concentration of 0.005% to 1%. After a 1-h incubation at room temperature, the reaction was quenched by adding 1 volume of 1 M glycine. The resultant protein preparations were separated by polyacrylamide gel electrophoresis with sodium dodecyl sulfate (SDS-PAGE) according to standard procedures.

Tissue Culture, Transfection, and Immunoblotting—The expression and immunoblot analysis were performed according to published protocols (13, 14).

Whole-cell Patch Clamp Recording—Whole-cell recordings were carried out according to a published protocol (5, 14, 15). A typical pulse protocol was designed according to the work of Smith *et al.* (5). After the gigaohm seal was achieved, the cell was first held at -77 mV, and the holding voltage was then jumped from this potential up to a long depolarizing potential of $+13$ mV for 600 ms, followed by decreasing test potentials from -57 mV to -137 mV at 20-mV increments. Current data were filtered at 1 kHz, digitized at 100- μs intervals, and stored in a computer (Dell 486/33) for later analysis. After basal leak current was subtracted, data were transferred to SigmaPlot (Jandel Scientific Software) for final analysis. The current density was then calculated from the capacitance of the recorded cells and the peak amplitude at -117 mV.

RESULTS AND DISCUSSION

One mutation found in patients with chromosome 7-linked long QT syndrome is a single-base deletion at 1261 ($\Delta 1261$), which introduces a frameshift at amino acid 421 of *HERG* (7). The resultant protein contains the first 420 amino acids of *HERG* (mostly its N-terminal hydrophilic domain), followed by a peptide of RLSSHPTRLPSK. The protein is truncated at amino acid position 432 because of a stop codon. In a heterozygotic patient, this mutation resulted in a dominant phenotype of cardiac sudden death (7). One possible cellular mechanism for this phenomenon is that the truncated $\Delta 1261$ protein might associate with the intact subunit to alter the expression or properties of the wild-type subunit. If this is the case, it is likely that there is an embedded region or regions in the $\Delta 1261$ protein for subunit interaction. Amino acid comparison of *HERG* and other *eag*-related genes has revealed significant homology, including a stretch within the N-terminal region (1). This conserved region, which we called *NAB_{HERG}*, corresponds to amino acids 1 to 135 in *HERG*.

Since topologically comparable regions in the Shaker-like K⁺ channels are involved in subunit assembly (12), it would be interesting to test whether this region is involved in subunit interaction as well. We expressed this coding fragment as a GST fusion protein in *Escherichia coli*. This fusion protein, with an apparent molecular weight of 39,700 (consistent with the predicted size), was affinity-purified on glutathione-Sepharose beads (Fig. 1A, lane 2). Since the GST portion and the conserved domain (*NAB_{HERG}*) are linked by a peptide containing a cleavage site for a sequence-specific proteinase, thrombin, the purified protein was digested with thrombin to yield two polypeptides (29.7 and 12.8 kDa) corresponding to the GST protein and *NAB_{HERG}* (Fig. 1A, lane 3). The thrombin digestion of this fusion protein was highly specific, since prolonged incubation with enzyme yielded no additional proteolytic species (Fig. 1A, lanes 3–6), and mock digestion revealed no detectable protein degradation (Fig. 1A, lane 7).

If the conserved *HERG* region is involved in subunit interaction, it may be sufficient to form oligomers in the absence of the rest of the protein, similar to other subunit assembly domains of Kv1 to Kv4 subfamilies of Shaker-like channels (17). To test this hypothesis, we separated the GST-*NAB_{HERG}* on a Superdex-200 gel filtration column by FPLC and developed the

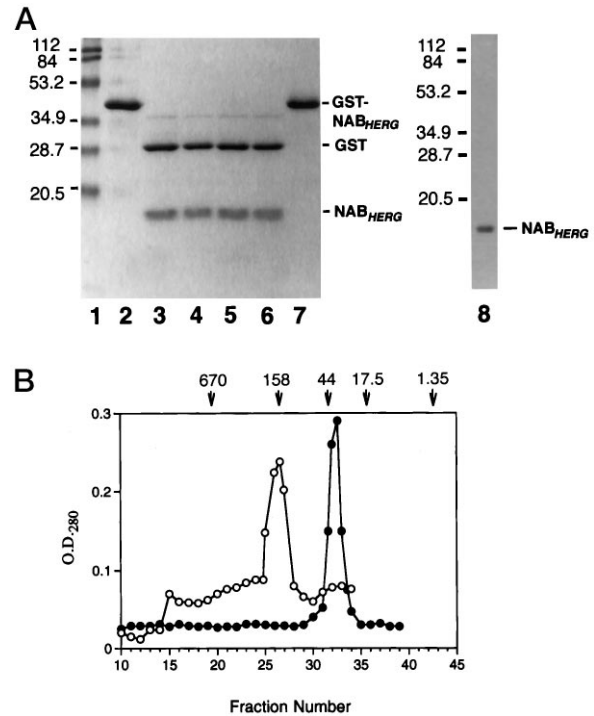


FIG. 1. Purified *NAB_{HERG}* proteins are oligomers. A, expression and purification of *NAB_{HERG}*. The GST-*NAB_{HERG}* fusion protein produced in *E. coli* was affinity-purified and digested with thrombin (see “Experimental Procedures”). The resultant polypeptides (about 0.5 μg per lane) were separated by polyacrylamide gel electrophoresis with SDS-PAGE (15% for lanes 1–7, 12.5% for lane 8) and visualized by Coomassie stain. Lanes 1 and 2 are prestained protein molecular weight markers (Bio-Rad) and purified GST-*NAB_{HERG}*. The GST-*NAB_{HERG}* fusion protein was treated with thrombin for 30 min (lane 3), 1 h (lane 4), 2 h (lane 5), and 4 h (lane 6). Lane 7 shows a 4-h mock digestion (with no thrombin added). To purify *NAB_{HERG}*, the digested GST-*NAB_{HERG}* was separated by fast-performance liquid chromatography (FPLC) on a Mono Q column. The purified *NAB_{HERG}* is shown in lane 8. B, gel filtration fractionation of GST-*NAB_{HERG}* and *NAB_{HERG}*. Superdex-200 was used to separate the purified fusion protein, and A_{280} profiles are shown. Open circles, GST-*NAB_{HERG}*; closed circles, *NAB_{HERG}*. Protein standards (in kDa) are thyroglobulin (670), bovine γ -globulin (158), chicken ovalbumin (44), equine myoglobin (17.5), and vitamin B₁₂ (1.35). Their migration positions on Superdex-200 are marked by arrows.

column under high-salt conditions (0.5 M NaCl) to reduce non-specific hydrophilic protein-protein interactions. The A_{280} chromatogram revealed a major peak corresponding to the Stoke’s radius of a 160-kDa globular protein (Fig. 1B, open circles). When protein in each fraction was separated by SDS-PAGE followed by silver staining, the major peak was indeed the purified GST-*NAB_{HERG}* protein (39.7 kDa). This result indicates that GST-*NAB_{HERG}* is an oligomer.

Since the GST portion of the fusion protein may contribute to the protein-protein interaction, we performed similar experiments using pure *NAB_{HERG}* protein (12.8 kDa) after purification on a Mono Q column (Fig. 1A, lane 8; also see “Experimental Procedures”). The A_{280} chromatogram of the Superdex-200 separation showed only a single *NAB_{HERG}* protein peak corresponding to a globular protein with a molecular weight of 40,000 (Fig. 1B, closed circles). Thus, oligomer formation is mediated by *NAB_{HERG}*.

The uniform migration profile of GST-*NAB_{HERG}* and *NAB_{HERG}* in the gel filtration column (Fig. 1B) supports the hypothesis that oligomers were formed via these specific interactions. Since both Shaker-like K⁺ channels and inward-rectifier K⁺ channels are tetramers (18–20), it is likely that the *HERG* homomultimeric channel also contains four subunits. To

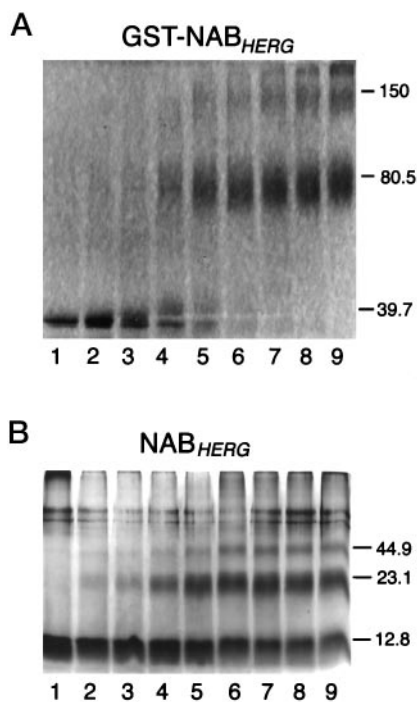


FIG. 2. Tetrameric complexes of *HERG* proteins as shown by chemical cross-linking. GST-NAB_{HERG} (A) and NAB_{HERG} (B) proteins were separated by polyacrylamide gel electrophoresis with sodium dodecyl sulfate after incubation with glutaraldehyde at the following concentrations: 1, 0.005%; 2, 0.01%; 3, 0.02%; 4, 0.04%; 5, 0.08%; 6, 0.1%; 7, 0.2%; 8, 0.4%; 9, 0.8%. Calculated molecular masses are marked on the right (in kDa). GST-NAB_{HERG} (A) and NAB_{HERG} (B) proteins were visualized by Coomassie stain and silver stain, respectively.

test whether the oligomers observed in gel filtration analysis are tetramers, we used either purified GST-NAB_{HERG} or NAB_{HERG} protein to perform chemical cross-linking experiments. Fig. 2A shows SDS-PAGE analysis of the GST-NAB_{HERG} protein (39.7 kDa) after incubation with different concentrations of glutaraldehyde (see “Experimental Procedures”). As the concentration was increased, two discrete additional protein species, with apparent molecular masses of 80.5 and 150 kDa (which agree with the sizes of dimers and tetramers), were detected. Similarly, when NAB_{HERG} (12.8 kDa) was subjected to the same analysis, we observed additional polypeptides with higher molecular masses of 23.1 and 44.9 kDa, which correspond to the sizes of dimers and tetramers (Fig. 2B). Taken together, these results showed that oligomeric NAB_{HERG} is a tetramer.

A region involved in subunit interaction may participate in several cellular processes including but not limited to subunit assembly. Depending on the detailed assembly pathway of a specific oligomeric protein, coexpression of a truncated form together with its intact subunit or subunits can result in inhibition of the expression of functional oligomers to different degrees, since the truncated protein can compete for subunit interaction. This dominant suppression in channel expression has been observed in transiently transfected cells that express the Shaker-like K^+ channels and the acetylcholine receptor (21, 22). Since sequence data indicate that the human $\Delta 1261$ mutation results in a truncated N-terminal domain of the *HERG* subunit, it would be particularly interesting to test whether this truncated protein containing NAB_{HERG} is capable of inhibiting the functional expression of *HERG*.

We expressed *HERG* in COS cells using conventional transient transfection procedures, and a whole-cell voltage clamp was used to record the characteristic current induced by *HERG*

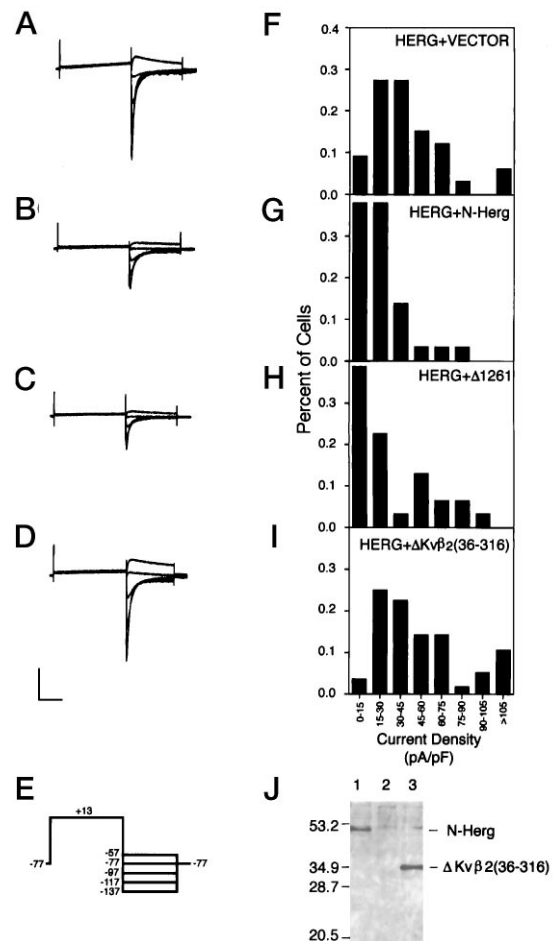


FIG. 3. Decrease of functional *HERG* expression by either N-Herg or $\Delta 1261$. Potassium current traces were recorded from COS cells that were transfected with four combinations of plasmids: *HERG* (5 μ g) + control plasmid (15 μ g) (panel A, $n = 33$), *HERG* (5 μ g) + N-Herg (15 μ g) (panel B, $n = 29$), *HERG* (5 μ g) + $\Delta 1261$ (15 μ g) (panel C, $n = 29$), and *HERG* (5 μ g) + $\Delta Kv\beta 2$ -(39–316) (15 μ g) (panel D, $n = 28$). One representative trace per group is shown. The test protocols are indicated at the bottom (panel E). Bars, 1000 pA and 200 ms. The current density for each recorded cell was calculated on the basis of the capacitance and the peak current (pA/pF) at -117 mV from the holding potential of $+13$ mV. Panels F–I are plots of current density (horizontal axis) versus percentage of cells (vertical axis). The expression of N-Herg (lane 1), $\Delta 1261$ (lane 2), and $\Delta Kv\beta 2$ -(39–316) (lane 3) was determined by immunoblot (panel J) using a monoclonal antibody 12CA5 (14). The expression of $\Delta 1261$ was low and not detectable.

(4, 5). The *HERG* channel was expressed alone or in the presence of either the N-terminal domain of *HERG* (N-Herg, amino acids 1 to 396) or $\Delta 1261$ (see “Experimental Procedures” for detailed amino acid positions). Within each group, we recorded from more than 29 transfected cells that expressed *HERG* currents. Consistent with previous results obtained in *Xenopus* oocytes, the electrophysiological properties of *HERG* channels showed no detectable changes in the presence or absence of truncated proteins (Fig. 3, A–D) (9).

When the current density within each group was determined and plotted against the number of cells in the percentage of cells, we found that either N-Herg or $\Delta 1261$ shifts the overall distribution of current density to a lower level (Fig. 3, E–H). The current densities for these three groups are 42.7 ± 4.95 pA/pF (mean \pm S.E., $n = 33$) for *HERG* + control plasmid, 29.1 ± 4.99 pA/pF (mean \pm S.E., $n = 29$) for *HERG* + $\Delta 1261$, and 22.5 ± 3.54 pA/pF (mean \pm S.E., $n = 29$) for *HERG* + N-Herg. Although transfection efficiency can vary by experiment, the distribution of current density among cells positive

for *HERG* current is relatively consistent between different experiments. The decrease of current density is not a result of alteration of cell surface area, since there is no significant difference in capacitance among the three groups. Therefore, both N-Herg and $\Delta 1261$ containing NAB_{HERG} do inhibit the expression of *HERG* ($p < 0.05$ for $\Delta 1261$ and $p < 0.001$ for N-Herg), presumably by competing for the functional subunit assembly of *HERG* channels. The decrease of current density of *HERG* channels could also result from nonselective inhibition by the NH_2 -terminal domain of *HERG*. To test this, we expressed *HERG* with $\Delta Kv\beta 2$ -(39–316), a truncated $Kv\beta 2$ subunit of Shaker-like potassium channel. Although the protein level of $\Delta Kv\beta 2$ -(39–316) is comparable to that of N-Herg and higher than that of $\Delta 1261$, $\Delta Kv\beta 2$ -(39–316) did not inhibit the expression of *HERG* (Fig. 3, *J* and *I*). To determine whether N-Herg and $\Delta 1261$ could nonspecifically inhibit surface expression of a membrane protein, we expressed membrane-bound CD_4 (a T-cell surface antigen) with N-Herg. Using fluorescence-activated cell sorting, we found comparable CD_4 surface expression in the presence or absence of N-Herg (data not shown). Taken together, these results support the idea that NAB_{HERG} plays a role in the subunit assembly of *HERG* channels. The decrease of current density by $\Delta 1261$ seen in the transfected cells may help explain the longer QT intervals seen in patients with the *HERG* mutations.

The Shaker-like K^+ channels and the *HERG* channels are clearly distinct classes of K^+ channels in terms of both amino acid sequence and electrophysiological properties. Although the region or regions that mediate subunit assembly of either *eag* or *eag*-related channels are not known, it has been shown that the N-terminal domains of Shaker-like channels play critical roles in specifying the formation of heteromultimers (12). Systematic analysis of subunit interaction of the four major subfamilies ($Kv1$ to $Kv4$) of Shaker-like K^+ channels has revealed the conserved motifs (NAB_{Kv1} to NAB_{Kv4}) for the subfamily-specific interaction (17). Despite no detectable homology between NAB_{HERG} and that of Shaker-like K^+ channels, the ability of NAB_{HERG} to form tetramers suggests remarkable similarity of assembly-domain arrangement between Shaker-like K^+ and *HERG* channels. Given that NAB_{HERG} has considerable homology to comparable regions in *eag* and *eag*-like potassium (*elk*) channels (1), it would be interesting to see whether these regions play a role in the subunit interaction of the corresponding channels.

The decrease in K^+ current density caused by either N-Herg or $\Delta 1261$ supports the notion that NAB_{HERG} participates in subunit assembly. One interesting question is why we did not observe a more dramatic decrease in current density. Several mechanisms may contribute to this apparent low-potency inhibition. From previous studies of Shaker-like K^+ channels and acetylcholine receptor, it is known that, in transfected cells, truncated subunits without transmembrane segments have much lower potency in suppressing functional channel expression than those with such segments (22). Since truncated fragments without membrane-spanning segments are more likely to be cytoplasmically soluble and non-membrane-bound, this difference was generally attributed to the potential difference in their targeting. In addition, both immunocytochemistry and immunoblot analyses have shown that $\Delta 1261$ expressed considerably less than N-Herg (Fig. 3*J*); yet $\Delta 1261$ and N-Herg in our assays have similar inhibition potency.

How could a mutated *HERG* subunit alter the channel activity in cardiac tissue to cause disease? A systematic approach to address this question would be to identify and examine all potential perturbations, including both loss and gain of a function, caused by the mutation. Perhaps a combination of changes alters certain aspects of cardiac function, which in concert contribute to cardiac sudden death. The effects of the $\Delta 1261$ mutant on *HERG* channel expression have previously been examined in a *Xenopus* oocyte system, and no suppression of channel expression was detected (9). It would be interesting to try to determine what accounts for the difference in expression between the mRNA-injected oocytes and the DNA-transfected mammalian tissue culture cells. Further, previous evidence has suggested that additional factors help define the I_{Kr} , since the *HERG* channel expressed in oocytes does not have the same pharmacological properties as I_{Kr} does. One interesting example is the *N*-methyl-D-aspartate receptor R1 (NR1), which by itself is capable of forming a functional glutamate receptor channel, with kinetic and pharmacological properties similar to those of native channels (23). However, more detailed molecular and biochemical analysis has revealed that the native *N*-methyl-D-aspartate receptors are in fact mostly heteromultimers of NR1, NR1 splice variants, and various NR2 subunits (24, 25). Thus, future biochemical analysis of the native *HERG* channel is essential to our understanding of the *HERG* function in the human heart.

Acknowledgments—We thank Dr. Mark Keating for *HERG* cDNA and Magdalena Bezanilla for N-Herg and $\Delta Kv\beta 2$ -(39–316) constructs. We also thank Drs. Daniel Raben and Peter Gillespie and members of the Li laboratory for helpful suggestions.

REFERENCES

- Warmke, J. W., and Ganetzky, B. (1994) *Proc. Natl. Acad. Sci. U. S. A.* **91**, 3438–3842
- Warmke, J., Drysdale, R., and Ganetzky, B. (1991) *Science* **252**, 1560–1562
- Drysdale, R., Warmke, J., Kreber, R., and Ganetzky, B. (1991) *Genetics* **127**, 497–505
- Trudeau, M. C., Warmke, J. W., Ganetzky, B., and Robertson, G. A. (1995) *Science* **269**, 92–95
- Smith, P. L., Baukrowitz, T., and Yellen, G. (1996) *Nature* **379**, 833–836
- Jan, L. Y., and Jan, Y. N. (1994) *Nature* **371**, 119–122
- Curran, M. E., Splawski, I., Timothy, K. W., Vincent, G. M., Green, E. D., and Keating, M. T. (1995) *Cell* **80**, 795–803
- Sanguinetti, M. C., Jiang, C., Curran, M. E., and Keating, M. T. (1995) *Cell* **81**, 299–307
- Sanguinetti, M. C., Curran, M. E., Spector, P. S., and Keating, M. T. (1995) *Proc. Natl. Acad. Sci. U. S. A.* **93**, 2208–2212
- Sambrook, J., Fritsch, E. F., and Maniatis, T. (1989) *Molecular Cloning*, 2nd Ed., Cold Spring Harbor Laboratory, Cold Spring Harbor, NY
- Ausubel, F. M., Brent, R., Kingston, R. E., Moore, D. D., Seidman, J. G., Smith, J. A., and Struhl, K. (1993) *Current Protocols in Molecular Biology*, Greene Publishing Associates and John Wiley & Sons, New York
- Li, M., Jan, Y. N., and Jan, L. Y. (1992) *Science* **257**, 1225–1230
- Jurman, M. E., Boland, L. M., Liu, Y., and Yellen, G. (1994) *Biotechniques* **17**, 876–881
- Yu, W. F., Xu, J., and Li, M. (1996) *Neuron* **16**, 441–453
- Hamill, O. P., Marty, A., Nehre, E., Sakmann, B., and Sigworth, F. J. (1981) *Pflügers Arch.* **391**, 85–100
- Barry, P. H. (1994) *J. Neurosci. Methods* **51**, 107–116
- Xu, J., Yu, W., Jan, Y. N., Jan, L. Y., and Li, M. (1995) *J. Biol. Chem.* **270**, 24761–24768
- Li, M., Unwin, N., Stauffer, K. A., Jan, Y. N., and Jan, L. Y. (1994) *Curr. Biol.* **4**, 110–115
- MacKinnon, R. (1991) *Nature* **350**, 232–235
- Yang, J., Jan, Y. N., and Jan, L. Y. (1995) *Neuron* **15**, 1441–1447
- Yu, X. M., and Hall, Z. W. (1991) *Nature* **352**, 64–67
- Tu, L., Santarelli, V., and Deutsch, C. (1995) *Biophys. J.* **68**, 147–156
- Moriyoshi, K., Masu, M., Ishii, T., Shigemoto, R., Mizuno, N., and Nakanishi, S. (1991) *Nature* **354**, 31–37
- Nakanishi, S. (1992) *Science* **258**, 597–603
- Hollmann, M., and Heinemann, S. (1994) *Annu. Rev. Neurosci.* **17**, 31–108